Progress In Electromagnetics Research, PIER 89, 275–289, 2009

WEAK FORM NONUNIFORM FAST FOURIER TRANSFORM METHOD FOR SOLVING VOLUME INTEGRAL EQUATIONS

Z. H. Fan, R. S. Chen, H. Chen, and D. Z. Ding

Department of Communication Engineering
Nanjing University of Science and Technology
Nanjing, Jiangsu 210094, China

Abstract—Electromagnetic scattering problems involving inhomogeneous objects can be numerically solved by applying a method of moment's discretization to the hypersingular volume integral equation in which a grad-div operator acts on a vector potential. The vector potential is a spatial convolution of the free space Green's function and the contrast source over the domain of interest. For electrically large problems, the direct solution of the resulting linear system is expensive, both computationally and in memory use. Conventionally, the fast Fourier transform method (FFT) combined Krylov subspace iterative approaches are adopted. However, the uniform discretization required by FFT is not ideal for those problems involving inhomogeneous scatterers and sharp discontinuities. In this paper, a nonuniform FFT method combined weak form integral equation technique is presented. The method performs better in terms of speed and memory use than FFT on the configuration involving both the electrically large and fine structures. This is illustrated by a representative numerical test case.

1. INTRODUCTION

The scattering of electromagnetic waves by objects of arbitrary shape is an important research subject. Pioneering works treating three dimensional arbitrary dielectric bodies are mainly based on the method of moment (MoM) [1, 2]. The MoM requires $O(N^2)$ computer memory and $O(N^3)$ computation time because of the need to store and invert the MoM matrix [3], where N is the number of

Corresponding author: Z. H. Fan (zhfan@mail.njust.edu.cn).

unknowns in the problem. An important improvement over the MoM is conjugate gradient — fast Fourier transform method (CG-FFT) [4–14]. It uses conjugate gradient algorithm (CG), one of the Krylov subspace iterative approaches [15], to solve the integral equation, and the required matrix-vector product during the iteration is efficiently evaluated by using the fast Fourier transform (FFT) scheme. Compared with the conventional method of moments, this iterative method is more efficient in terms of the required computer memory and computation time. In FFT solution, the computer memory and computation time requirements are $O(N)$ and $O(KN \log N)$, respectively, where K is the number of Krylov subspace iterations. In spite of the success of these Krylov-subspace iterative FFT methods, they all require a uniform distribution of the grid points due to the use of the regular FFT algorithms. This uniform discretization is not ideal for those problems involving inhomogeneous scatterers and sharp discontinuities. In particular, when the medium involves both electrically large and small regions, the FFT method needs to discretize the problem with a very fine grid in order to accommodate a detailed description of the electrically small regions. Therefore, the method wastes an unnecessarily large number of unknowns for electrically large regions. To overcome this restriction, the nonuniform fast Fourier transform (NUFFT) algorithm is introduced [16–20]. In [16], the NUFFT is combined with the CG method for one- and two-dimensional problems with transverse magnetic wave incidence. However, NUFFT algorithm is difficult to be directly applied for the case of two-dimensional problems with transverse electric wave incidence and three-dimensional problems due to the existing of the higher order singularity of the dyad Green's function in the integral equations. In this article, we adopt the idea of the weak-form integral equations introduced in [21, 22], which leads to a weaker singularity in the Green's function, to overcome this restriction. Both FFT and NUFFT algorithms reduce the CPU time to $O(N \log_2 N)$ and computer memory to $O(N)$ [23–26], much smaller than $O(N^2)$ by the MoM. However, the NUFFT method gives the important flexibility of nonuniform sampling and maintains the computational efficiency of the conventional FFT method. The poor convergence for iterative solution is observed when the nonuniform sampling is employed. In this work, we use Morgan's deflated restarting generalized minimal residual method (DRGMRES) [27] to mitigate this problem, and present a combination of DRGMRES and NUFFT algorithms to solve the three dimensional volume integral equations.

2. THEORY

2.1. NUFFT

The considered problem is the fast evaluation of [18, 23, 24]

$$H(i) = \sum_{m=-M/2}^{M/2-1} h_m e^{j2\pi i v_m} \quad i = -\frac{N}{2}, -\frac{N}{2}+1, \ldots, \frac{N}{2}-1 \tag{1}$$

With $j = \sqrt{-1}$ denotes imaginary unit and $v_m \in (-1/2, 1/2)$. In matrix vector notation this reads

$$H = Ah \tag{2}$$

where A is the $N \times M$ nonequispaced Fourier matrix with the element $A_{im} = e^{j2\pi i v_m}$. H and h are two vectors with length N and M, respectively. The straightforward algorithm for computing this matrix vector product is called non-uniform discrete Fourier transform (NUDFT). A closely related matrix vector product is the adjoint NUDFT

$$\hat{h}_m = \sum_{i=-N/2}^{N/2-1} \hat{H}(i) e^{-j2\pi i v_m} \tag{3}$$

$$\hat{h} = A^H \hat{H} \tag{4}$$

where A^H denotes the conjugate transpose of the nonequispaced Fourier matrix A. The NUDFT and the adjoint NUDFT take $O(MN)$ arithmetical operations. Using NUFFT calculation technique, denoting as $A = \mathbf{F}_1(h)$ and $\hat{h} = \mathbf{F}_1^H(\hat{H})$, the computation of (1) and (3) can reduce to $O(N \log N + mM)$ arithmetic operations. For more details, the reader can read the references [18, 23-27] for the detailed knowledge of the non-uniform FFT.

2.2. Volume Integral Equation

We consider the computation of the scattering field from an inhomogeneous dielectric body to illustrate the application of the NUFFT-based method in three dimensions. The medium surrounding the dielectric body is free space and an $e^{j\omega t}$ dependence is assumed and suppressed for the field expressions. As shown in Fig. 1, an object is illuminated by an incident electric field $\mathbf{E}^i$ with angular frequency ω and the inhomogeneous body is characterized by permittivity $\varepsilon_r(\mathbf{r})\varepsilon_0$,

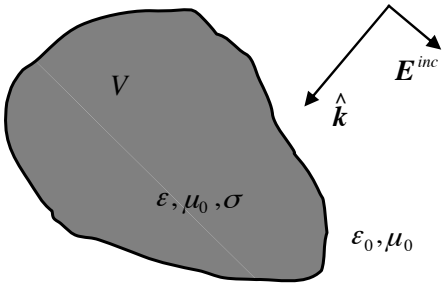

Figure 1. A three dimensional lossy dielectric object placed in free space illuminated by a plane electromagnetic wave with $\hat{k}$-direction incidence.

electric conductivity $\sigma(\mathbf{r})$ and permeability μ_0, here ε_0 and μ_0 denote the permittivity and permeability in free space, respectively.

The corresponding volume integral equation [1, 2, 21, 28] can be written as

$$\mathbf{E}(\mathbf{r}) - \mathbf{E}^i(\mathbf{r}) = \mathbf{E}^s(\mathbf{r}) = \left(k_0^2 + \nabla\nabla\right) \cdot \mathbf{A}(\mathbf{r}), \quad r \in V \tag{5}$$

with $k_0 = \omega\sqrt{\mu_0\varepsilon_0}$ is free space wavenumber, and the magnetic vector potential is computed as

$$\mathbf{A}(\mathbf{r}) = \frac{1}{j\omega\varepsilon_0} \int_V G(\mathbf{r}, \mathbf{r}')\mathbf{J}(\mathbf{r}')dV'. \tag{6}$$

G is the free space Green's function given by

$$G(\mathbf{r}, \mathbf{r}') = \frac{\exp(-jk_0|\mathbf{r} - \mathbf{r}'|)}{4\pi|\mathbf{r} - \mathbf{r}'|} \tag{7}$$

and the equivalent volume current density $\mathbf{J}$, which also is called as contrast source, can be expressed using electric flux density $\mathbf{D}$:

$$\mathbf{J}(\mathbf{r}) = j\omega\left[\varepsilon(\mathbf{r}) - \varepsilon_0\right]\mathbf{E}(\mathbf{r}) = j\omega\chi(\mathbf{r})\mathbf{D}(\mathbf{r}) \tag{8}$$

with

$$\varepsilon(\mathbf{r}) = \varepsilon_r(\mathbf{r})\varepsilon_0 - j\frac{\sigma(\mathbf{r})}{\omega} \text{ and } \chi(\mathbf{r}) = \frac{\varepsilon(\mathbf{r}) - \varepsilon_0}{\varepsilon(\mathbf{r})} \tag{9}$$

From above equations, it can be found that Equation (1) is actually a Fredholm integral equation of the second kind for the unknown electric flux density $\mathbf{D}$.

$$\mathbf{E}^i(\mathbf{r}) = \frac{\mathbf{D}(\mathbf{r})}{\varepsilon(\mathbf{r})} - (k_0^2 + \nabla\nabla) \cdot \int_V G(\mathbf{r}, \mathbf{r}')\frac{\chi(\mathbf{r}')}{\varepsilon_0}\mathbf{D}(\mathbf{r}')dV', \quad \mathbf{r}' \in V \tag{10}$$

Once (10) is solved for $\mathbf{D}$ in V by use of method of moments, Equation (5) can be used to calculate the scattered field everywhere in space.

2.3. Weak form Testing and Expansion Procedure

From (5) and (10), we can see that the problem of electromagnetic scattering by a three-dimensional dielectric object can be formulated in terms of a hypersingular integral equation, in which a grad-div operator acts on a vector potential $\mathbf{A}$. The vector potential $\mathbf{A}$ is a spatial convolution of the free space Green's function G and the contrast source $\mathbf{J}$ over the domain of interest. As in [21, 22], a weak form of the integral equation for the relevant unknown quantity is obtained by testing it with appropriate testing functions. Then the vector potential is expanded in a sequence of the appropriate expansion functions and the grad-div operator is integrated analytically over the scattering object domain only. The spatial convolution can be carried out numerically using nonuniform discrete Fourier transforms.

The three dimensional rooftop basis functions are used to discrete the electric flux density $\mathbf{D}$ and the magnetic vector potential $\mathbf{A}$. It is worthwhile to note that we discrete the electric flux density $\mathbf{D}$ which only resides the space of nonzero electric current $\mathbf{J}$ despite it is practically nonzero in the whole space.

The scatterer domain is embedded in a rectangular block with a dimension $L_x \times L_y \times L_z$, we discretize this block into non-uniform cuboid cells. To convert (10) into a matrix equation, we expand the electric flux density and the vector potential in (5) as

$$\mathbf{D}(\mathbf{r}) = \varepsilon_0 \sum_{q=1}^{3} \sum_{u,v,w} d_q^{uvw} \mathbf{f}_q^{uvw}(\mathbf{r}) \tag{11}$$

$$\mathbf{A}(\mathbf{r}) = \sum_{q=1}^{3} \sum_{u,v,w} a_q^{uvw} \mathbf{f}_q^{uvw}(\mathbf{r}) \tag{12}$$

where $\mathbf{f}_1^{uvw}$, $\mathbf{f}_2^{uvw}$, and $\mathbf{f}_3^{uvw}$ are vector volumetric rooftop functions in the x-, y-, and z-directions, respectively. Defined as in [21, 22], d_q^{uvw} and a_q^{uvw} are the value of the q component of the electric flux density and the vector potential at the center of the rooftop functions. With this choice for the basis functions, the normal component of $\mathbf{D}$ is continuous across all facets of the grid, as required by the boundary conditions. Furthermore, the contrast function χ is approximated by a piecewise constant function which assumes one value per cell. Note that the boundary condition of $\mathbf{A}$ is different from the case of the $\mathbf{J}$. $\mathbf{A}$

has nonzero value in whole space while the contrast source $\mathbf{J}$ vanishes outside the object. Hence in our analysis, the mesh volume should be larger than the object's volume since it requires the differential of $\mathbf{A}$ to join the computation.

We then take the Garlerkin technique by testing (5) with $\mathbf{f}_p^{mnk}(\mathbf{r})$ ($p = 1, 2, 3$). We note the relationship

$$\int_V \mathbf{f}_p^{mnk}(\mathbf{r}) \cdot \nabla\nabla \cdot \mathbf{A}(\mathbf{r}) dV = \int_V \nabla \cdot \left[\mathbf{f}_p^{mnk}(\mathbf{r}) \nabla \cdot \mathbf{A}(\mathbf{r})\right] dV - \int_V \nabla \cdot \mathbf{f}_p^{mnk}(\mathbf{r}) \nabla \cdot \mathbf{A}(\mathbf{r}) dV \quad (13)$$

where $\nabla \cdot \mathbf{A}(\mathbf{r})$ is defined by Lorenz gauge condition and equals to $j\omega\mu_0\varepsilon_0\phi$ and ϕ is scalar electric potential which is continuously differentiable. Using the divergence theorem and the continuity of the normal components of ϕ through the interfaces between these subdomains, we obtain

$$\int_V \nabla \cdot \left[\mathbf{f}_p^{mnk}(\mathbf{r}) \nabla \cdot \mathbf{A}(\mathbf{r})\right] dV = \oint_S \left[\mathbf{f}_p^{mnk}(\mathbf{r}) \nabla \cdot \mathbf{A}(\mathbf{r})\right] \cdot d\mathbf{S} = 0 \quad (14)$$

Hence, we can transfer one del operator from $\mathbf{A}(\mathbf{r})$ to $\mathbf{f}_p^{mnk}(\mathbf{r})$. The Garlerkin procedure can be expressed as

$$\int_V \mathbf{f}_p^{mnk}(\mathbf{r}) \cdot \left(\frac{\mathbf{D}(\mathbf{r})}{\varepsilon(\mathbf{r})} - k_0^2 \mathbf{A}(\mathbf{r})\right) dV + \int_V \nabla \cdot \mathbf{f}_p^{mnk}(\mathbf{r}) \nabla \cdot \mathbf{A}(\mathbf{r}) dV = \int_V \mathbf{f}_p^{mnk}(\mathbf{r}) \cdot \mathbf{E}^{inc}(\mathbf{r}) dV \quad (15)$$

This is a linear equation group of a_q^{mnk} and d_q^{mnk} written as

$$Pa + Qd = e. \quad (16)$$

It is not difficult to find that P, Q are sparse matrices with dimensions $N \times N$; e is a vector with length N. The relationship between a_q^{mnk} and d_q^{mnk} can be determinate by discretizing the following equation.

$$\mathbf{A}(\mathbf{r}) = \frac{1}{\varepsilon_0} \int_V G(\mathbf{r}, \mathbf{r}') \chi(\mathbf{r}') \mathbf{D}(\mathbf{r}') dV' \quad (17)$$

Note that the integral in (17) is a convolution one, thus it can be calculated utilizing two continuous forward three-dimensional Fourier transforms and one continuous inverse three-dimensional Fourier transform

$$\mathbf{A} = \frac{1}{\varepsilon_0} \mathbf{F}^{-1} \left\{\mathbf{F}\left[G\right] \cdot \mathbf{F}\left[\chi \mathbf{D}\right]\right\} \quad (18)$$

where $\mathbf{F}$ and $\mathbf{F}^{-1}$ denote the forward and inverse Fourier transform, respectively. It can be calculated using the NUDFT technique and can be accelerated by NUFFT algorithm.

2.4. Fast Calculation of Convolution Using NUFFT

For the clarity, we take example for one dimensional convolution. In this scenario, it is to compute:

$$h(x) = \int_a^b g\left(x - x'\right) f\left(x'\right) dx' \tag{19}$$

where the function f has a finite support of $[a, b]$ and the function g has an infinite support. Let $x = t + \frac{a+b}{2}$, we can get

$$h\left(t + \frac{a+b}{2}\right) = \int_{-\frac{L}{2}}^{\frac{L}{2}} g(t - t') f(t') dt' = \frac{1}{2\pi} \int_{-\infty}^{\infty} G(\omega) F(\omega) e^{-j\omega t} d\omega \tag{20}$$

For a function $f(t)$ with a support $t \in [-L/2, L/2]$, $L = \frac{b-a}{2}$, the one dimensional continuous Fourier transform is defined as

$$F(\omega) = \int_{-L/2}^{L/2} f(t) \exp(j\omega t) dt. \tag{21}$$

We expand $f(t)$ with a series of basis functions $B_m(t)$, where B_m represents Lagrangian interpolation functions. Using the pulse function

$$B_m(t) = \begin{cases} 1, & \text{if } t \in D_m \\ 0, & \text{otherwise} \end{cases} \tag{22}$$

as a basis, we have

$$F(\omega) = \sum_{m=-M/2}^{M/2-1} f(t_m) \cdot \int_{D_m} B_m(t) \exp(j\omega t) dt \tag{23}$$

where $D_m = \left[t_m - \frac{\Delta t_m}{2}, t_m + \frac{\Delta t_{m+1}}{2}\right]$ is the support of $B_m(t)$. Here, t_m is the mth location of the sampling points and Δt_m is the distance between t_m and t_{m-1}. The relationship among t_m, Δt_m and D_m are shown in Fig. 2. Sampling the frequency domain and letting $\omega = \frac{2\pi}{L} i$, $i = -N/2, \ldots, N/2 - 1$, we obtain

$$F(i) \approx \mathbf{F}_1(f) = \sum_{m=-M/2}^{M/2-1} \Delta t_m f(t_m) \exp\left[j \frac{2\pi}{L} i t_m\right] \tag{24}$$

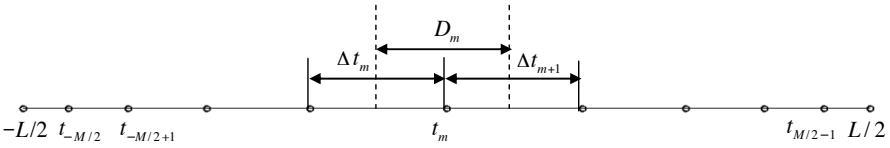

Figure 2. The discretization parameters for one dimensional nonuniform fast Fourier transform.

It results in the definition of a nonuniform discrete Fourier transform (NUDFT) of M points as in (1). In a similar way, the Fourier transform of the Green's function g, denoted as $G(i)$, can be calculated by NUFFT algorithms. It is worthwhile to point out that the discretizations of the space-domain Green's function and the electric flux density can be in disagreement, but in the Fourier-transform domain they are required to coincide with each other. The arithmetic operation for NUFFT algorithms to compute the above convolution is $O(N \log_2 N)$, asymptotically the same as the regular FFT algorithms. However, it has a promising property of nonuniform sampling. Note that, in order to perform the linear convolution through DFT in (19), the truncation support of the Green's function should be $[-L', L']$, $L' > L$, and the above NUFFT lengths are $M_g \geq 2M$ and the above NUFFT lengths are $N \geq 2M$. Once $F(i)$ and $G(i)$ are obtained, $h(t_m)$ can be calculated by use of the trapezoid rule with a truncation, that is,

$$h(t_m) \approx \frac{1}{L} \sum_{i=-N/2}^{N/2-1} G(i)F(i)e^{-j\frac{2\pi}{L}it_m} \qquad m = -\frac{M}{2}, \ldots, \frac{M}{2} \tag{25}$$

It can be accelerated using adjoint NUFFT algorithms.

$$h = \frac{1}{L}\mathbf{F}_1^H \left\{\mathbf{F}_1 [g] \cdot \mathbf{F_1} [f]\right\} \tag{26}$$

From the above analysis, it is easy to obtain the relationship between A_q^{mnk} and d_q^{mnk} by

$$a_q^{mnk} = \frac{1}{\varepsilon_0 L_x L_y L_z}\mathbf{F}_1^H \left\{\mathbf{F}_1 [G] \cdot \mathbf{F_1} \left[\chi^{mnk} d_q^{mnk}\right]\right\} \tag{27}$$

Note that the NUFFT for the Green's function needs to be done only once in the implementation. Substituting (27) into (15), we can obtain a linear equation group regarding d_q^{mnk} written as

$$Q'd = e \tag{28}$$

This can be iteratively solved with Krylov-subspace iterative methods, where the matrix-vector product operation is efficiently evaluated by using NUFFT algorithms. Therefore, the NUFFT retains the computational efficiency of the FFT combined with Krylov-subspace iterative methods, but gives the important flexibility of nonuniform sampling. As expected, the nonuniform discretization leads to a slow convergence rate. In this paper, a modified version of restart generalized minimal residual method (GMRES), called DRGMRES, is chosen to improve the convergence rate. It deflates the eigenvalues with the smallest moduli by adding the corresponding harmonic Ritz eigenvectors into the Krylov subspace. Deflation can significantly improve the convergence of restarted GMRES, and it helps robustness by allowing the solution of many tough problems that have small eigenvalues.

3. NUMERICAL RESULTS

We firstly consider a homogeneous dielectric cuboid with side length $L_x = L_y = 0.3\,\mathrm{m}$, $L_z = 0.6\,\mathrm{m}$, and relative permittivity $\varepsilon_r = 4.0$. The cuboid center is located at the original point as shown in Fig. 3. The incident plane wave is with the operating frequency at 300 MHz and with the incident angules $\theta^i = 180^\circ$ and $\phi^i = 0^\circ$. In order to validate our three dimensional NUFFT algorithms, the cuboid is discretized with $16 \times 16 \times 32$ grids, nonuniformly distributed in both x and y directions as shown in Fig. 4 and uniformly in z direction. The results for the bistatic radar cross section (RCS) of the cuboid are given in Fig. 3, and are compared with the solutions using the weak-form FFT method in [13], which uses equispaced knots. It can be easily found that our numerical results have an excellent agreement with the weak-form FFT method. This serves to verify our DRGMRES-NUFFT implementation.

In the second case, we consider an inhomogeneous dielectric cube coated with another dielectric material, which is shown in Fig. 5. The dielectric cube has size length of $L = 3\,\mathrm{m}$ and its relative permittivity and conductivity are $\varepsilon_{r1} = 8.0$, $\sigma_1 = 0.0030$; the thin coated layer has the thickness $a = 0.0328\,\mathrm{m}$ and its relative permittivity and conductivity are $\varepsilon_{r2} = 4.0$, $\sigma_2 = 0.0050$. The incident plane wave is with the operating frequency at 100 MHz and incident angules $\theta^i = 180^\circ$ and $\phi^i = 0^\circ$. If conventional iterative FFT method is applied, in order to make sure that there are two grid points located inside the coating by use of a uniform discretization, a total of $183 \times 183 \times 183$ grids should be needed, and it overloads the common personal computer. However, only $32 \times 32 \times 32$ grids are required when a nonuniform

discretization is employed, where two grid points are put inside the outer coated layer and 30 grids are equally distributed for the inner region. Applying NUFFT algorithms, the memory requirement is 187 times less than the regular FFT algorithms. While the in our cases, the computational cost of each NUFFT is twice as fast as the FFT with the same node [18, 19, 23–26]. Therefore, large memory and computational cost can be saved due to the flexibility of nonuniform sampling of NUFFT algorithms. The bistatic RCS results of the coated cube are displayed in Fig. 4.

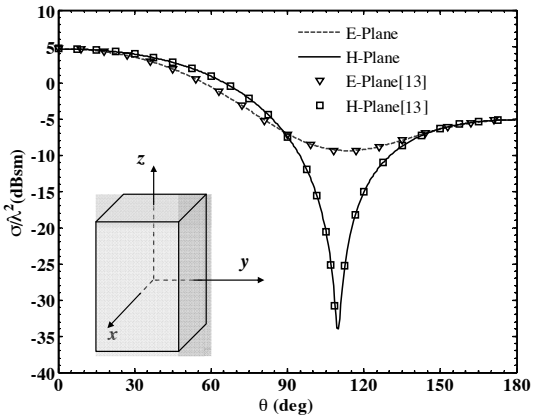

Figure 3. Bistatic RCS of the homogeneous dielectric cuboid problem.

Figure 4. The nonuniform nodes distribution of the x- and y-direction discretization for the homogeneous dielectric cuboid problem.

Figure 6 shows the convergence histories of GMRES-, BCGSTAB-, TFQMR-, and DRGMRES-NUFFT methods, we refer the readers to [12, 15, 29–32] for the details of the GMRES, BCGSTAB, TFQMR iterative methods. In this case, the dimension of the subspace for both GMRES and DRGMRES is set to be 30, and 8 approximate eigenvectors are used in DRGMRES [27] to improve convergence. The initial guess solution vectors for these iterative methods are all set as zero vectors. The average CPU time for one matrix-vector product (MVP) operation is 11.95 second. It can be easily found that both BCGSTAB and TFQMR do not reach convergence within the

maximum 5000 iterations. The number of MVPs to reach convergence is 1591 for GMRES and 804 for DRGMRES, and the CPU time is 19080.4 second and 9867.1 second for them, respectively. It is found that about two times improvement is achieved for DRGMRES when compared with the conventional restarted GMRES in terms of MVPs. When measured in terms of CPU time, the same improvement can also be obtained. This justifies the use of approximate eigenvectors for deflated restarting for GMRES method.

Finally, we investigate the sensitivity of the convergence of DRGMRES to the parameter k, which is the number of approximate

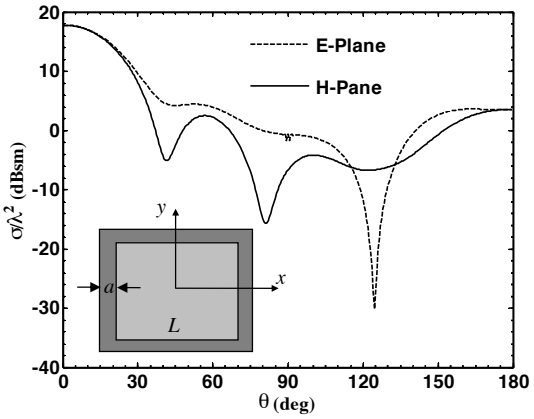

Figure 5. Bistatic RCS of the coated dielectric cube problem.

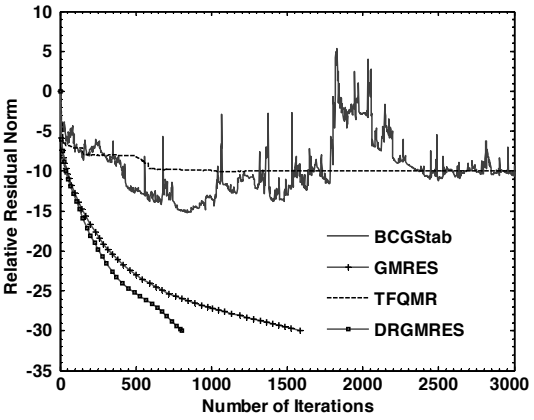

Figure 6. Convergence histories of various methods for the coated cube problem.

eigenvectors used for deflated restarting. To address this issue, the coated cube problem described above is investigated again. Fig. 7 displays the varying convergence property of DRGMRES with respect to the number of approximate eigenvectors k. It should be noted that when no eigenvectors are used (i.e., $k = 0$) DRGMRES is reduced to the standard restarted GMRES method. As shown in Fig. 5, the number of MVPs gradually decreases as k increases from 0 to 8. This indicates that with a small number of eigenvectors for deflated restarting, the convergence rate of the conventional GMRES method can be greatly improved. However, as k goes increase to 20, almost the same convergence is obtained. This is mainly because the gain by using the approximate eigenvectors compensates the reduction in the dimension of Krylov-subspace of DRGMRES, which, however, inhibits convergence.

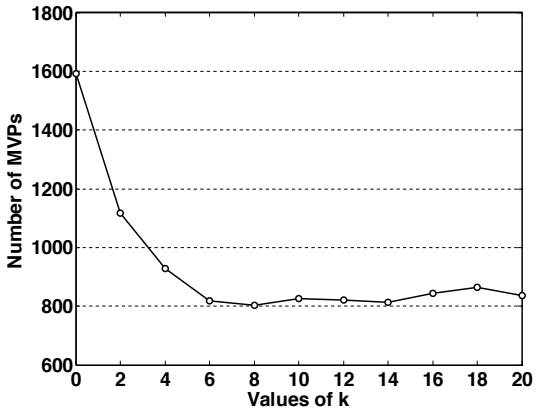

Figure 7. Sensitivity of the convergence of DRGMRES to the parameter k for the coated cube problem.

4. CONCLUSIONS

In this paper, the deflated restarting GMRES (DRGMRES) iterative method, combined with the weak form nonuniform FFT (NUFFT) algorithms, is proposed to solve three dimensional volume electric field integral equations in electromagnetic scattering problems. Numerical experiments for problems involving both electrically large and fine regions are conducted, which shows the advantage of the NUFFT over the conventional FFT methods and the efficiency of DRGMRES for improving convergence of the standard GMRES.

ACKNOWLEDGMENT

The authors would like to thank the assistance and support of Natural Science Foundation of China under Contract Number 60701003, 60431010 and China Postdoctoral Science Foundation under Contract Number 20070411053, Jiangsu Planned Projects for Postdoctoral Research Funds under Contract Number 0701020C.

REFERENCES

1. Livesay, D. E. and K. M. Chen, "Electromagnetic fields induced inside arbitrarily shaped biological bodies," *IEEE Trans. on MTT*, Vol. 22, 1273–1280, 1974.
2. Schaubert, D., D. Wilton, and A. Glisson, "A tetrahedral modeling method for electromagnetic scattering by arbitrarily shaped inhomogeneous dielectric bodies," *IEEE Transactions on Antennas and Propagation*, Vol. 32, No. 1, 77–85, 1984.
3. Davidson, D. B., *Computational Electromagnetics for RF and Microwave Engineering*, Cambridge University Press, Apr. 2005.
4. Nie, X.-C., N. Yuan, L.-W. Li, T. S. Yeo, and Y.-B. Gan, "Fast analysis of electromagnetic transmission through arbitrarily shaped airborne radomes using precorrected-FFT method," *Progress In Electromagnetics Research*, PIER 54, 37–59, 2005.
5. Li, L.-W., Y.-J. Wang, and E.-P. Li, "MPI-based parallelized precorrected FFT algorithm for analyzing scattering by arbitrarily shaped three-dimensional objects," *Progress In Electromagnetics Research*, PIER 42, 247–259, 2003.
6. Volakis, J. L. and K. Barkeshli, "Applications of the conjugate gradient FFT method to radiation and scattering," *Progress In Electromagnetics Research*, PIER 05, 159–239, 1991.
7. Peterson, A. F., S. L. Ray, C. H. Chen, and R. Mittra, "Numerical implementations of the conjugate gradient method and the CG-FFT for electromagnetic scattering," *Progress In Electromagnetics Research*, PIER 05, 241–300, 1991.
8. Gago, E. and M. F. Catedra, "Analysis of finite sized conducting patches in multilayer media using the CG-FFT method and discretizing Green's function in the spectral domain," *Progress In Electromagnetics Research*, PIER 05, 301–327, 1991.
9. Gan, H. and W. C. Chew, "A discrete BCG-FFT algorithm for solving 3D inhomogeneous scatterer problems," *Journal of Electromagnetic Waves and Applications*, Vol. 9, 1339–1357, 1995.
10. Xin, Y. F. and P.-L. Rui, "Adaptively accelerated GMRES fast

fourier transform method for electromagnetic scattering," *Progress In Electromagnetics Research*, PIER 81, 303–314, 2008.

11. Rui, P.-L. and R.-S. Chen, "Implicitly restarted GMRES fast Fourier transform method for electromagnetic scattering," *Journal of Electromagnetic Waves and Applications*, Vol. 21, No. 7, 973–986, 2007.
12. Fan, Z. H., D. X. Wang, R. S. Chen, and E. K. N. Yung, "The application of iterative solvers in discrete dipole approximation method for computing electromagnetic scattering," *Microwave and Optical Technology Letters*, Vol. 48, No. 9, 1741–1746, Sep. 2006.
13. Rui, P. L., R. S. Chen, Z. H. Fan, E. K. N. Yung, C. H. Chan, Z. Nie, and J. Hu, "Fast analysis of electromagnetic scattering of 3-D dielectric bodies with augmented GMRES-FFT method," *IEEE Transactions on Antennas and Propagation*, Vol. 53, No. 11, 3848–3852, Nov. 2005.
14. Zhao, L., T.-J. Cui, and W.-D. Li, "An efficient algorithm for EM scattering by electrically large dielectric objects using MR-QEB iterative scheme and CG-FFT method," *Progress In Electromagnetics Research*, PIER 67, 341–355, 2007.
15. Saad, Y., *Iterative Methods for Sparse Linear Systems*, PWS, Publishing Company, 1996.
16. Xu, X. M. and Q. H. Liu, "Conjugate-gradient nonuniform fast Fourier transform (CG-NUFFT) method for one- and two-dimensional media," *Microwave and Optical Technology Letters*, Vol. 24, No. 6, 385–389, 2000.
17. Liu, Q. H. and X. Y. Tang, "Iterative algorithm for nonuniform inverse fast Fourier transform (NU-IFFT)," *Electronics Letters*, Vol. 34, No. 20, 1913–1914, Oct. 1, 1998.
18. Liu, Q. H. and N. Nguyen, "Accurate algorithm for nonuniform fast Fourier transforms (NUFFT's)," *IEEE Microwave and Guided Wave Letters*, Vol. 8, No. 1, 18–20, Jan. 1998.
19. Liu, Q. H., X. M. Xu, B. Tian, and Z. Q. Zhang, "Applications of nonuniform fast transform algorithms in numerical solutions of differential and integral equations," *IEEE Transactions on Geoscience and Remote Sensing*, Vol. 38, No. 4, Part I, 1551–1560, July 2000.
20. Liu, Q. H., X. M. Xu, and Z. Q. Zhang, "Applications of nonuniform fast transform algorithms in numerical solutions of integral equations," *Annual Review of Progress in Applied Computational Electromagnetics*, Vol. 2, 897–904, 2000.

21. Zwamborn, P. and P. M. van den Berg, "The three-dimensional weak form of the conjugate gradient FFT method for solving scattering problems," *IEEE Transactions on Microwave Theory and Techniques*, Vol. 40, No. 9, 1757–1766, 1992.
22. Zhang, Z. Q. and Q. H. Liu, "Three-dimensional weak-form conjugate- and biconjugate-gradient FFT methods for volume integral equations," *Microwave and Optical Technology Letters*, Vol. 29, No. 5, 350–356, 2001.
23. Potts, D. and G. Steidl, "Fast summation at nonequispaced knots by NFFTs," *SIAM J. on Sci. Comput.*, Vol. 24, 2013–2037, 2003.
24. Dutt, A. and V. Rokhlin, "Fast Fourier transforms for nonequispaced data," *SIAM J. Sci. Stat. Comput.*, Vol. 14, 1368–1393, 1993.
25. Kunis, S. and D. Potts, "Time and memory requirements of the Nonequispaced FFT," *Sampling Theory in Signal and Image Processing*, Vol. 7, 77–100, 2008.
26. Fessler, J. A. and B. P. Sutton, "Nonuniform fast Fourier transforms using min-max interpolation," *IEEE Transactions on Signal Processing*, Vol. 51, No. 2, 560–574, Feb. 2003.
27. Morgan, R. B., "GMRES with deflated restarting," *SIAM J. Sci. Comput.*, Vol. 24, 20–37, 2002.
28. Jin, J. M., *The Finite Element Method in Electromagnetics*, 2nd edition, John Wiley & Sons, New York, 2002.
29. Chen, R. S., Z. H. Fan, and E. K. N. Yung, "Analysis of electromagnetic scattering of three-dimensional dielectric bodies using Krylov subspace FFT iterative methods," *Source: Microwave and Optical Technology Letters*, Vol. 39, No. 4, 261–7, Nov. 20, 2003.
30. Ding, D.-Z., R.-S. Chen, and Z. Fan, "An efficient SAI preconditioning technique for higher order hierarchical MLFMM implementation," *Progress In Electromagnetics Research*, PIER 88, 255–273, 2008.
31. Fan, Z., D.-Z. Ding, and R.-S. Chen, "The efficient analysis of electromagnetic scattering from composite structures using hybrid CFIE-IEFIE," *Progress In Electromagnetics Research B*, Vol. 10, 131–143, 2008.
32. Carpentieri, B., "Fast large RCS calculation using the boundary element method," *Journal of Electromagnetic Waves and Applications*, Vol. 21, No. 14, 1959–1968, 2007.